Title:

Enhanced network synchronization connectivity following transcranial direct current stimulation (tDCS) in bipolar depression: effects on EEG oscillations and deep learning-based predictors of clinical remission

Authors:

Wenyi Xiao [a], Jijomon C. Moncy [a], Ali-Reza Ghazi-Noori [a], Rachel D. Woodham [a], Hakimeh Rezaei [a, b], Elvira Bramon [c], Philipp Ritter [b], Michael Bauer [b], Allan H. Young [d, e, f], Cynthia H.Y. Fu [a, d, f]

Affiliations:

a) School of Psychology, University of East London, London, UK
b) Technische Universität Dresden, Dresden, Germany
c) Department of Psychiatry, University College London, London, UK
d) Centre for Affective Disorders, Department of Psychological Medicine, Institute of Psychiatry, Psychology and Neuroscience, King's College London, London, UK
e) National Institute for Health Research Biomedical Research Centre at South London and Maudsley NHS Foundation Trust, King's College London, London, UK
f) South London and Maudsley NHS Foundation Trust, Bethlem Royal Hospital, Beckenham, UK

Authors for correspondence:

Dr. Wenyi Xiao, University of East London, School of Psychology, Arthur Edwards Building, Water Lane, London E15 4LZ, UK
Tel : +44 (0)208 223 4119, Email : wxiao@uel.ac.uk

Professor CHY Fu, University of East London, School of Psychology, Arthur Edwards Building, Water Lane, London E15 4LZ, UK
Tel : +44 (0)208 223 4119, Email : c.fu@uel.ac.uk, cynthia.fu@kcl.ac.uk

Abstract

Aim: To investigate oscillatory networks in bipolar depression, effects of a home-based tDCS treatment protocol, and potential predictors of clinical response.

Methods: 20 participants (14 women) with bipolar disorder, mean age 50.75 ± 10.46 years, in a depressive episode of severe severity (mean Montgomery-Åsberg Rating Scale (MADRS) score 24.60 ± 2.87) received home-based transcranial direct current stimulation (tDCS) treatment for 6 weeks. Clinical remission defined as MADRS score < 10. Resting-state EEG data were acquired at baseline, prior to the start of treatment, and at the end of treatment, using a portable 4-channel EEG device (electrode positions: AF7, AF8, TP9, TP10). EEG band power was extracted for each electrode and phase locking value (PLV) was computed as a functional connectivity measure of phase synchronization. Deep learning was applied to pre-treatment PLV features to examine potential predictors of clinical remission.

Results: Following treatment, 11 participants (9 women) attained clinical remission. A significant positive correlation was observed with improvements in depressive symptoms and delta band PLV in frontal and temporoparietal regional channel pairs. An interaction effect in network synchronisation was observed in beta band PLV in temporoparietal regions, in which participants who attained clinical remission showed increased synchronisation following tDCS treatment, which was decreased in participants who did not achieve clinical remission. Main effects of clinical remission status were observed in several PLV bands: clinical remission following tDCS treatment was associated with increased PLV in frontal and temporal regions and in several frequency bands, including delta, theta, alpha and beta, as compared to participants who did not achieve clinical remission. The highest deep learning prediction accuracy 69.45% (sensitivity 71.68%, specificity 66.72%) was obtained from PLV features combined from theta, beta, and gamma bands.

Conclusions: tDCS treatment enhances network synchronisation, potentially increasing inhibitory control, which underscores improvement in depressive symptoms. Baseline EEG-based measures might aid predicting clinical response.

Highlight

- Investigated EEG-based functional connectivity in bipolar depression and effects of home-based tDCS treatment on clinical response predictors.

- Improved depressive symptoms correlated with delta band phase locking value (PLV), indicating enhanced EEG synchronization.

- Increased beta band PLV in temporoparietal regions for participants achieving clinical remission, contrasting with decreased PLV in non-remissions from baseline to post-treatment.

- Heightened synchronization in delta, theta, alpha and beta band PLV observed in participants achieving clinical remission post-treatment.

- Deep learning predicted treatment response with 69.45% accuracy using baseline PLV features from theta, beta, and gamma bands.

1. Introduction

Bipolar disorder (BP) is characterized by episodes of elevated mood states as well as depressive and mixed mood states that are associated with changes in sleep and appetite, energy levels, and psychomotor activity (American Psychiatric Association, 2013). Treatment for bipolar depression usually involves medications, such as mood stabilisers and antipsychotic medication, which may be combined with psychotherapy. However, these treatments have limited effectiveness, in part related to individual differences in treatment response and high rates of discontinuation due to intolerability and adverse effects (Chakrabarti, 2014; McIntyre et al., 2022).

The non-invasive brain stimulation, transcranial direct current stimulation (tDCS), is a potential treatment option for bipolar depression (Mutz et al., 2018, 2019, Woodham et al., 2021). tDCS generates a weak direct current (0.5 - 2.0 mA) which is applied to the scalp through electrodes. In bipolar depression, the anode electrode is usually placed over the left dorsolateral prefrontal cortex (DLFPC) and cathode electrode over the right DLPFC, frontotemporal or suborbital region (Tortella et al., 2015; Mutz et al., 2018, 2019). The current modulates resting membrane potential, in which anode stimulation increases neuronal excitability with a reduction in GABAergic activity while cathode stimulation decreases neuronal excitability by reducing glutamate levels (Stagg et al., 2018). tDCS does not lead to neuronal depolarisation, in contrast to repetitive transcranial magnetic stimulation (rTMS), and it does not lead to a generalised seizure, in contrast to electroconvulsive therapy (ECT). tDCS stimulation has been found to modulate functional interactions in brain networks extending beyond the regions directly targeted by stimulation, impacting on the wider neural network underlying mood regulation (Polania et al., 2011; Kunze et al., 2016; Woodham et al., 2021).

 Meta-analyses have reported clinical efficacy for a course of active tDCS treatment as compared to sham tDCS treatment in bipolar depression and unipolar depression (major depressive disorder) in randomised controlled trials (Mutz et al., 2019; Hsu et al., 2024) and that longer treatment durations show greater clinical efficacy (Nikolin et al., 2023). tDCS treatment involves daily sessions over several weeks, and initial studies had been conducted in clinical research settings, requiring participants to commit to daily commutes (Mutz et al., 2019). As tDCS is portable and safe, it can be provided at home (Woodham et al., 2021). Self-administered, home-based tDCS affords greater flexibility to patients and is more cost effective than clinic-administered tDCS. We developed a remotely supervised, home-based tDCS

protocol, which has demonstrated strong clinical outcomes, high acceptability and feasibility in open-label trials in bipolar depression (Ghazi-Noori et al., 2024) and unipolar depression (Woodham et al., 2022), as well as clinical efficacy and safety in a multisite randomized controlled trial in unipolar depression (Woodham et al., 2023).

The DLPFC is a key region in emotion processing and executive functioning, which are impaired in bipolar depression (Hassel et al., 2008; Townsend et al., 2010). Imbalances in activity in the left and right DLPFC, namely hypoactivity in the left DLPFC and hyperactivity in the right DLPFC, has been found in depression (Grimm et al., 2008; Maeda et al., 2000). The prefrontal cortex has a crucial role in regulating responses to threat by directly inhibiting the amygdala complex, in which electrical stimulation over the prefrontal cortex inhibits amygdala response (Quirk et al., 2003).

Oscillations in electrical activity between brain regions range from slow to fast frequencies, which reflect coupling between regions during different states and in mental health disorders. Synchronization in oscillatory networks underlies the variable affective states in bipolar disorder (Chen et al., 2008, Kam et al., 2013). Electroencephalography (EEG) provides a measure of electrical activity in brain regions, generating assessments of the strength and connections between regions.

In bipolar disorder, increased power in high frequency bands, namely beta and gamma, has been observed as compared to healthy participants (Kam et al., 2013). In bipolar depression though, reductions in the high frequency beta/gamma bands have been reported (Canali et al., 2015), and increasing depressive severity was associated with decreased gamma band synchronization (Kim et al., 2013). Following rTMS treatment, clinical response was associated with increased strength in EEG functional connectivity, as measured by beta and gamma phase locking value (PLV) in frontal region and temporal-parietal regions in bipolar depression (Zuchowicz et al., 2019). Moreover, increased power in low frequency delta and theta bands at baseline was associated with a subsequent clinical response to rTMS in unipolar and bipolar depression (Woźniak-Kwaśniewska et al., 2015). However, oscillatory network synchronization following tDCS treatment has not been examined in bipolar depression. Furthermore, by applying data-driven artificial intelligence algorithms, we may be able to develop predictors of clinical response (Fu and Costafreda, 2013).

In the present study, we sought to investigate the oscillatory networks in bipolar depression, effects of a home-based tDCS treatment protocol, and potential predictors of clinical response. We utilized a portable wireless EEG device with 4-dry electrodes which has demonstrated robust signal properties (Cannard et al., 2021; Krigolson et al., 2021), participants underwent EEG acquisition in their own homes with real-time supervision by video conference. We investigated EEG metrics, namely power and PLV, associated with changes in depressive severity as well as the categorial effects of clinical remission. To explore preliminary EEG-based predictors, we applied deep learning to examine whether baseline EEG measures could predict clinical remission, expecting that oscillations in low-frequency bands might be predictive of treatment outcomes, as suggested by previous rTMS studies (Woźniak-Kwaśniewska et al., 2015).

2. Methods

2.1. Participants

Ethical approval was provided by London Fulham Research Ethics Committee. All participants provided written informed consent electronically. The study was an open-label, single arm acceptability and feasibility trial of home-based tDCS treatment for bipolar depression (Ghazi-Noori et al., 2024). Participants were aged 18 years or above, with a diagnosis of bipolar disorder and in a current major depressive episode without psychotic features, based on Diagnostic and Statistical Manual of Mental Disorders, Fifth Edition (DSM-5) (American Psychiatric Association, 2013), determined by a structured assessment using the Mini-International Neuropsychiatric Interview (MINI; Version 7.2) (Sheehan et al., 1998). All participants had at least a moderate severity of depressive symptoms, as measured by a minimum score of 18 on the Montgomery-Åsberg Depression Rating Scale (MADRS) (Montgomery and Åsberg 1979). Participants were either medication-free or taking a stable regime of mood-stabilizing medication or in psychotherapy for a minimum of two weeks. Exclusion criteria included significant suicide risk, comorbid psychiatric disorder, and contraindications to tDCS. Ghazi-Noori et al. (2024) provides a full description of the study.

2.2. tDCS treatment protocol

The protocol consisted of a 6-week course of active tDCS, which was self-administered by participants in their homes 5 times a week for 3 weeks and then twice a week for 3 weeks, for a total of 21 sessions. A member of the research team was present at each session by Microsoft Teams video call to monitor adherence to the protocol and to ensure safe use of the device as this was a feasibility trial. The tDCS headset devices were sent to participants and training was provided via the associated app and by research team members.

A bifrontal montage was applied with the anode positioned over left DLPFC (F3 position according to international 10/20 EEG system) and cathode over right DLPFC (F4 position). Each electrode was a $23cm^2$ conductive rubber electrode covered by saline soaked sponges. Simulation was 2 mA for a duration of 30 minutes with a gradual ramp up over 120 seconds at the start and ramp down over 15 seconds at the end of each session. The Flow Neuroscience tDCS device was used for all participants.

Clinical assessments included clinician-rated measures of depressive symptoms, MADRS and Hamilton Depression Rating Scale (HDRS-17) (Hamilton, 1960), anxiety symptoms: Hamilton Anxiety Rating Scale (HAMA) (Hamilton, 1959) and manic symptoms: YMRS (Young et al., 1978); self-report measure of depressive symptoms: Patient Health Questionnaire-9 (PHQ-9) (Kroenke et al., 2001), disability and impairment: Sheehan Disability Scale (SDS) (Sheehan, 1893) and Quality of Life Enjoyment and Satisfaction Questionnaire (Q-LES-Q) (Endicott et al., 1993). Clinical remission was defined as the MADRS score of less than 10 at the end of the treatment.

2.3. Remote EEG acquisition and preprocessing

EEG data were acquired at two time points: at baseline, prior to the start of treatment (pre-treatment), and at the end of treatment (post-treatment). EEG data had been acquired in a sub-sample of 22 participants (15 women; mean age 51.59 years) at baseline, however, data were not available for one participant post-treatment and data from another participant was of poor quality and was not included. Thus, data were available in 20 participants (14 women; mean age 50.75 years, SD 10.46 years), at pre-treatment and post-treatment (Table 1).

At each EEG acquisition session, a trained research team member provided real-time guidance via videoconference. At each EEG session, four 5-minute EEG recordings were acquired. Each

recording measured at resting state in which participants were asked to maintain a relaxed posture without any body movements. The resting state recordings were conducted in the following order: eyes closed, eyes open, eyes closed, and eyes open. The two five-minutes resting state eyes-closed recording at pre- and post-treatment were used the present analysis.

EEG recordings were acquired using a Muse device, a wireless EEG device equipped with 4 dry electrodes (Figure 1). Sampling frequency was 256 Hz. Frontal electrode positions were AF7 and AF8, and the temporoparietal positions were TP9 and TP10. EEG signals were referenced to the FPz electrode.

Each recording was segmented into 60 separate EEG windows, each lasting 10 seconds without overlap. The recorded EEG signals, saved in CSV format, included timestamps for each EEG sample, raw EEG signals from each electrode, Horse Shoe Indicator (HSI) values for each electrode. HSI values served as indicators of electrode connectivity quality: HSI value 1 indicates excellent connectivity between electrode and the participant's scalp, 2 indicates average connectivity, and 4 poor connectivity. Values were averaged across the samples in each window, and all windows with an average HSI of 2 or less were selected.

Each EEG signal was segmented into 10-second windows. EEG signals from each electrode undergo filtering across six distinct frequency bands: the full band (1-60 Hz), delta δ (1-4 Hz), theta θ (4-8 Hz), alpha α (8-12 Hz), beta β (12-30 Hz), and gamma γ (30-60 Hz). Employing Butterworth Infinite Impulse Response (IIR) filters of 5th order, the signals are effectively filtered.

2.4. EEG analysis

EEG band power and phase locking value (PLV) were extracted as resting state EEG metrics. EEG band power was calculated for all four electrodes (AF7, AF8, TP9, TP10). PLV was computed for all possible electrode pairs (AF7-AF8, AF7-TP9, AF7-TP10, AF8-TP9, AF8-TP10, TP9-TP10). PLV assesses the phase synchrony between two time series signals (Hoke et al., 1989; Lachaux et al., 1999). It is a common measure employed to determine functional connectivity between EEG signals recorded from two electrodes, offering insight into the temporal relationships of neural signals independent of their amplitude. PLV is a metric constrained within the range of 0 to 1. PLV value approaching 1 indicates high phase synchronization with minimum variation in phase difference across the EEG signals, while a

value close to 0 suggests no phase synchronization. The phase difference is obtained from the instantaneous phase of the signal, which is determined using the signal and its Hilbert transform. Since the instantaneous phase cannot be directly associated with a specific frequency band or single frequency, we first applied band-pass filtering to the EEG signal to isolate the respective EEG frequency bands. Subsequently, we calculated the PLV values within these specific frequency bands. A total of 24 band power values and 36 PLVs were computed with two sets of 60 EEG measurements at pre- and post- treatment, were available for statistical analysis. Full description is presented in Supplementary Materials.

2.5. Statistical analyses

Statistical analyses of band power and PLV were performed to investigate potential associations between changes in EEG measures and depression severity and to assess effects of remission and non-remission status following tDCS treatment.

Non-parametric tests were utilized due to concerns about distributional assumptions. Specifically, the Mann-Whitney U test was used for between-group comparisons (remission vs. non-remission), and Spearman's rank correlation analysis was conducted to examine the relationship between changes in EEG measures and the proportional change in MADRS scores from baseline to the end of the 6-week treatment period, across all participants. The proportional change in MADRS is calculated by subtracting the baseline MADRS score from the MADRS score after 6 weeks of treatment, then dividing this absolute difference by the baseline MADRS score.

Factorial analyses with and without proportional change in MADRS as covariate were used for between-group comparisons. A two-way ANOVA, supplemented with non-parametric tests, was performed for each EEG variable to test whether EEG measures change in response to treatment. The factors were: remission group (remission, non-remission) and Time (baseline pre-treatment, post-treatment). A total of 60 statistical tests were performed.

The coefficients were estimated in the R statistical environment (R core team, 2021) using linear regression (*lm* built-in function). Post hoc tests (Tukey honestly significant difference (HSD)) were performed to assess significant effects. The statistical threshold was set at $p<0.05$, with

correction for multiple comparisons by controlling False Discovery Rate (FDR). A full description is in the supplementary materials.

2.6. Deep learning analysis

Participants were categorized into two groups based on their remission status following tDCS treatment. In the classification analysis, remission was defined as the positive class and non-remission as the negative class, with sensitivity representing remission and specificity representing non-remission. Values were extracted from each EEG frequency band at pre-treatment.

From each EEG band, PLV feature vectors with a dimensionality of 6 are generated, representing each of the six electrode pairs. These six-dimensional feature vectors, both individually and through the concatenation of PLV features from multiple EEG bands, were employed as inputs for deep learning models with varying parameters. This concatenation process at the feature level led to a linear increase in the feature dimension. To assess the effectiveness of different combinations of PLV features from individual bands and combinations of multiple bands, two distinct deep learning architectures were investigated. The first architecture utilized a fully connected perceptron deep learning structure, and the second employed a one-dimensional convolutional neural network (1DCNN) architecture. Considering combination of features from multiple EEG bands, the dimensionality varied as follows: 6 (single band), 12 (two-band combination), 18 (three-band combination), 24 (four-band combination), and 30 (combination of all bands).

For the fully connected perceptron deep learning network, a four-layer architecture was implemented, comprising layers with 32, 32, 16, and 1 perceptrons (output layer) for all input combinations, except in the case of the all-band combination where the feature size was 3. In this scenario, 64 perceptrons were employed in the first layer. The all-band combination encompassed all PLV features extracted from the delta to gamma bands. In the 1DCNN-based architecture, the initial fully connected layer of the perceptron network was replaced with a convolutional layer. This convolutional layer employed a kernel size of 3. To ensure kernel overlap, the number of filters used was determined by multiplying the input dimension by a multiplication factor 2/3. Following the convolutional layer, a MaxPooling1D layer with a pool size of 2 was integrated to downsample the feature maps, aiming to extract the most relevant

features while reducing computational complexity. For single-band PLV features with an input dimension of 6, 4 filters with a kernel size of 3 were used. Similarly, for dimensions 12, 18, 24, and 30, 8, 12, 16, and 20 filters were employed respectively. The activation function 'relu' was applied to all layers except the output layer, where 'sigmoid' was utilized. To minimize the 'binary cross-entropy' loss function, the 'adam' optimizer was employed.

Due to the constrained size of the dataset and our emphasis on accurately evaluating model performance over computational efficiency, we opted for the Leave-One-Subject-Out (LOSO) methodology to assess the deep learning model's accuracy. Employing this approach, we conducted 20 iterations of training and testing for each input combination. During each iteration, one participant out of the 20 was reserved for testing, while the PLV features from the remaining 19 participants were utilized for model training. Following 50 epochs of model training, we identified the most effective model based on its classification accuracy on a validation set. This validation set, comprising 240 randomly selected vectors, equally distributed between remission and non-remission groups, was drawn from the training data. The model exhibiting the highest classification accuracy on the validation set underwent further testing.

3. Results

3.1. Clinical outcome

Following tDCS treatment, 11 participants attained clinical remission (mean MADRS score post-treatment 5.18, SD 1.72) and 9 participants were in non-remission (mean MADRS score post-treatment 14.40, SD 4.88), which was a significant difference (t = -5.429, p < 0.001). In the remission group, significant improvements were observed across all clinical assessments; post-treatment scores were as follows: HDRS-17 (mean 3.55, SD 1.44), HAMA (mean 3.82, SD 1.66), YMRS (mean 0.64, SD 1.03), PHQ-9 (mean 5.27, SD 3.04), and SDS (mean 8.64, SD 6.28). In contrast, in the non-remission group, the post-treatment scores were higher: HDRS-17 (mean 10.56, SD 5.00), HAMA (mean 10.33, SD 4.06), YMRS (mean 1.33, SD 1.22), PHQ-9 (mean 10.56, SD 5.22), and SDS (mean 17.11, SD 6.47). Clinical outcomes for the full sample of participants in the study are reported in Ghazi-Noori et al. (2024). All participants remained on the same course of mood stabilizer and/or antidepressant medication for the duration of the trial and no participants started a new antidepressant treatment during the trial.

3.2. Relationship between changes in depression severity and EEG power

No significant correlation was found between change in EEG power and proportional change in MADRS scores from pre- to post-treatment (non-parametric analysis: Spearman's rank correlation).

3.3. Relationship between changes in depression severity and EEG PLV connectivity

Positive correlations with an improvement in depressive symptoms following tDCS treatment were found in full band PLV in several electrode pairs: AF8-TP9 ($\rho = 0.52$, FDR-adjusted $p = 0.02$), and TP9-TP10 ($\rho = 0.57$, FDR-adjusted $p = 0.01$), as well as in beta PLV in pair: AF7-AF8 ($\rho = 0.48$, FDR-adjusted $p = 0.03$) (non-parametric analysis: Spearman's rank correlation) (Figures 3, Supplementary Table 5). No regions showed a negative correlation with an improvement in depressive symptoms.

3.4. Effects of remission status in EEG power

A significant main effect of the group was observed in several EEG power regions and frequency bands. Specifically, in full power, significant effects were found in the TP10 region ($F = 4.77$, FDR-adjusted $p = 0.04$). In delta power, a significant effect was observed in the AF8 region ($F = 7.44$, FDR-adjusted $p = 0.01$). For beta power, significant effects were noted in the AF7 ($F = 7.28$, FDR-adjusted $p = 0.01$) and TP9 ($F = 5.84$, FDR-adjusted $p = 0.02$) regions. In gamma power, significant effects were present in the AF7 ($F = 5.72$, FDR-adjusted $p = 0.02$) and TP10 ($F = 8.93$, FDR-adjusted $p = 0.01$) regions (Supplementary Table 1).

Post-hoc tests revealed that only the TP9 region in the beta power band showed a significant post-treatment difference between the remission and non-remission groups (non-parametric analysis: Mann-Whitney U test, $U = 78.00$, FDR-adjusted $p = 0.03$). Other regions did not show significant post-treatment differences (Supplementary Table 2).

3.5. Effects of remission status in EEG PLV connectivity

A significant main effect of group was observed in full band PLV in AF7-TP10 ($F = 6.52$, FDR-adjusted $p = 0.02$), AF8-TP10 ($F = 11.86$, FDR-adjusted $p = 0.00$) and TP9-TP10 ($F = 8.43$,

FDR-adjusted p = 0.01). When examining the indices for the five frequency bands separately, significant main effects of group were observed in PLV in the following channel pairs: in delta band: AF7-AF8 (F = 5.39, FDR-adjusted p = 0.03), AF7-TP10 (F = 5.95, FDR-adjusted p = 0.02) and TP9-TP10 (F = 4.47, FDR-adjusted p = 0.04); in theta band: AF7-AF8 (F = 4.96, FDR-adjusted p = 0.03), AF8-TP9 (F = 4.71, FDR-adjusted p = 0.04) TP9-TP10 (F = 4.61, FDR-adjusted p = 0.04); in alpha band: AF7-AF8 (F = 6.48, FDR-adjusted p = 0.02), AF7-TP10 (F = 7.39, FDR-adjusted p = 0.01) and AF8-TP9 (F = 5.68, FDR-adjusted p = 0.02); in gamma band: AF8-TP10 (F = 5.10, FDR-adjusted p = 0.03), TP9-TP10 (F = 5.43, FDR-adjusted p = 0.03) (Supplementary Table 1). Post-hoc tests demonstrated that for each electrode pair, remission group showed a significantly higher PLV as compared to non-remission group (non-parametric analysis: Mann-Whitney U test) (Figure 4, Supplementary Table 2).

A significant main effect of time was found in the gamma band: PLV AF8-TP9 (F = 8.64, FDR-adjusted p = 0.01), in which there was decreased PLV post-treatment as compared to pre-treatment (Supplementary Table 1)

A significant interaction effect of remission group by time was found in the beta band PLV TP9-TP10 (F = 4.46, FDR-adjusted p = 0.04), in which there were no differences between the remission and non-remission groups at baseline, however remission group showed an increase in PLV from baseline to post-treatment while the non-remission group showed a significant decrease from baseline to post-treatment (Figure 5, Supplementary Table 1).

Post-hoc analyses were conducted for each significant variable identified, and the outcomes are presented in Supplementary Table 2. Importantly, we focus on the variables that show significant group differences at post-treatment, but not at baseline. Specifically, BP remission group have a generally greater PLV value compared to the BP non-remission group at the post-treatment, including PLV of AF7-AF8 in delta, theta and alpha bands (U_{delta} = 80, FDR-adjusted p = .02; U_{theta} = 81, FDR-adjusted p = .02; U_{alpha} 87, FDR-adjusted p = .00); PLV of AF7-TP10 in delta and alpha bands (U_{delta} = 77, FDR-adjusted p = .04; U_{beta} = 76, FDR-adjusted p = .02); PLV of TP9-TP10 in delta and theta(U_{delta} = 79, FDR-adjusted p = .03; U_{theta} = 81, FDR-adjusted p = .02) (non-parametric analysis: Mann-Whitney U test) (Figure 4, Supplementary Table 2).

3.6. Within group effects over time in remission and non-remission groups

In the remission group, a significant decrease in gamma band PLV AF8-TP9 was observed from baseline to post-treatment ($U = 54$, FDR-adjusted $p = 0.04$). Conversely, in the non-remission group, a significant decrease in beta band PLV TP9-TP10 was found from baseline to post-treatment ($U = 40$, FDR-adjusted $p = 0.04$) (Figure 2, Supplementary Table 3).

3.7. Deep learning-based prediction

The fully connected perceptron deep learning architecture, characterized by its fully connected layers, demonstrated superior performance metrics relative to the architecture predicated on a 1D-CNN. The fully connected perceptron architecture framework results are presented. Among the single EEG band PLV features, the highest classification accuracy of 62.2% was achieved for the alpha band (sensitivity 59.24%, specificity of 65.82%), and the beta band yielded the second highest classification accuracy of 59.93% (sensitivity of 68.94%, specificity 48.91%). In combinations of two band PLV, the theta-beta combination yielded the highest classification accuracy of 68.66% (sensitivity 73.85%, specificity 62.33%), and in the second highest accuracy was generated in the alpha-beta band feature combination accuracy 66.43% (sensitivity 74.52%, specificity 57.16%). Three band PLV combinations also exhibited high performance, particularly the combination of theta, beta, and gamma bands: accuracy 69.45% (sensitivity 71.68%, specificity 66.72%) and delta, alpha, and beta bands: accuracy 67.93% (sensitivity 74.49%, specificity 59.91%). In four band PLV combination, theta, alpha, beta, gamma combination yielded the highest classification accuracy 67.29% (sensitivity 72.78%, specificity 60.58%) and the second highest classification accuracy 66.02% (sensitivity 73.37%, specificity 57.02%) for delta, alpha, beta, gamma. While combining PLV features from all the five classical EEG bands delta, theta, alpha, beta, and gamma, we obtained an accuracy 66.57 (sensitivity 68.24%, specificity 64.53%) (Supplementary Table 4).

4. Discussion

We investigated the relationship between EEG measures of brain activity and clinical outcomes to a home-based tDCS protocol in bipolar depression and whether baseline EEG measures could predictors of clinical remission to tDCS treatment. We examined EEG power and functional connectivity, as measured by PLV which quantifies phase interdependencies between brain regions.

We found a significant positive correlation with improvements in depressive symptoms and the delta band PLV in frontal and temporoparietal regional channel pairs. The delta band is a low frequency EEG oscillation which is associated with cognitive control and enhanced internal concentration (Harmony et al., 2013). An interaction effect in network synchronisation was observed in beta band PLV in temporoparietal regions, in which participants who attained clinical remission showed increased synchronisation following tDCS treatment, which was decreased in participants who did not achieve clinical remission. Additionally, remission status significantly impacted beta power in the temporoparietal region, with differences observed post-treatment. Beta band activity, a higher frequency oscillation, is associated with response preparation and inhibitory control, whereby increased inhibitory controls leads to increased beta band activity (Zhang et al., 2008; Tzagarakis et al., 2010). These findings suggest that that tDCS treatment enhances network synchronisation, potentially increasing inhibitory control, which underscores the improvement in depressive symptoms (Pellegrino et al., 2018).

Additional main effects of group were observed in several PLV frequency bands. In particular, participants who attained clinical remission following tDCS treatment showed increased PLV in channel pairs in frontal and temporal regions and in several frequency bands, including delta, theta, alpha and beta as compared to participants who did not achieve clinical remission following tDCS treatment. The present findings are consistent with reports of rTMS treatment in bipolar depression, in which PLV is increased across multiple channel pairs and in several frequency bands, namely theta, alpha, and beta bands, in participants who show a clinical remission as compared to participants with who did not attain a clinical remission (Zuchowicz et al., 2019). Increased theta and delta band activity in prefrontal and temporparietal regions has also been reported following rTMS treatment in bipolar depression in participants who showed a clinical remission (Woźniak-Kwaśniewska et al., 2015). In contrast, participants who did not attain clinical remission following tDCS treatment showed a significant decrease in beta PLV, indicative of impaired neural phase synchronization, as compared to the participants who had attained clinical remission. Decreased synchronization in beta band was reported in bipolar disorder associated with cognitive impairments (Chen et al., 2008). The present findings indicate that there are underlying neural synchronizations in bipolar depression that can distinguish clinical response to tDCS.

Applying deep learning, we sought to explore whether we could predict clinical remission based on baseline PLV features. Deep learning is a form of artificial intelligence that uses neural

networks, which consists of a series of layers, to learn a representation of the data. The prediction accuracy ranged from 60-69%, while sensitivity values were generally higher, up to 76%. The highest prediction accuracy 69.45% was obtained for the combination of PLV features from the EEG bands theta, beta, and gamma with a balanced of sensitivity 71.68% and specificity of 66.72%. This finding aligns with another resting state EEG PLV analysis, in which the best classification performance for bipolar disorder was the beta band phase-synchronized feature (Duan et al., 2021). At the present time, we do not have any biomarkers that can help to identify and predict clinical responses. In unipolar depression, deep learning approaches have generated aggregate accuracies in the range of 70-80% for prediction of response to antidepressant medications, as measured by area under the curve (Squarcina et al., 2021). The findings suggest that adding a simple EEG measure at baseline can aid in identifying patients who will subsequently attain clinical remission following tDCS treatment, and in turn, this could identify patients who may not benefit from tDCS or who may require a combination of treatments.

The present study has several limitations. As the sample size was small and all participants had received active tDCS treatment, the power to detect a significant effect was limited and we cannot establish whether the findings are related to active or to placebo, sham effects. EEG data were acquired from four channels in a portable device which limited spatial resolution. We sought to include an easy-to-use device which participants could use at home that has strong reliability, research grade EEG data, and generates robust frequency measures comparable to a 64-channel device (Cannard et al., 2021; Krigolson et al., 2021). The EEG data were acquired in a resting state, while a cognitive task might have provided additional sensitivity in identifying predictors of clinical response (Mitoma et al., 2022).

In summary, tDCS treatment enhances network synchronisation, in particular in delta and beta bands, potentially increasing inhibitory control, which underscores improvement in depressive symptoms. Deep learning prediction models showed a range in which sensitivity values were generally higher, indicating that EEG-based measures might aid predicting clinical response.

References

Alonzo, A., Fong, J., Ball, N., Martin, D., Chand, N., & Loo, C., 2019. Pilot trial of home-administered transcranial direct current stimulation for the treatment of depression. J. Affect. Disord. 252, 475–483. https://doi.org/10.1016/j.jad.2019.04.041

American Psychiatric Association, D., & Association, A.P., 2013. Diagnostic and statistical manual of mental disorders: DSM-5 (Vol. 5, Issue 5). American psychiatric association Washington, DC. https://doi.org/10.1016/j.pnpbp.2023.110752

Borrione, L., Cavendish, B.A., Aparicio, L.V.M., Luethi, M.S., Goerigk, S., Carneiro, A.M., Valiengo, L., Moura, D.O., de Souza, J. P., Baptista, M., Aparecida da Silva, V., Klein, I., Suen, P., Gallucci-Neto, J., Padberg, F., Razza, L.B., Vanderhasselt, M.-A., Lotufo, P.A., Bensenor, I. M., … Brunoni, A.R., 2024. Home-use transcranial direct current stimulation for the treatment of a major depressive episode: A randomized clinical trial. JAMA Psychiatry. 81(8), 329-337. https://doi.org/10.1001/jamapsychiatry.2023.4948

Canali, P., Sarasso, S., Rosanova, M., Casarotto, S., Sferrazza-Papa, G., Gosseries, O., Fecchio, M., Massimini, M., Mariotti, M., & Cavallaro, R., 2015. Shared reduction of oscillatory natural frequencies in bipolar disorder, major depressive disorder and schizophrenia. J. Affect. Disord. 184, 111–115. https://doi.org/10.1016/j.jad.2015.05.043

Cannard, C., Wahbeh, H., & Delorme, A., 2021. Validating the wearable MUSE headset for EEG spectral analysis and Frontal Alpha Asymmetry. 2021 IEEE International Conference on

Bioinformatics and Biomedicine (BIBM). 3603–3610.
https://doi.org/10.1101/2021.11.02.466989

Chakrabarti, S., 2014. What's in a name? Compliance, adherence and concordance in chronic
psychiatric disorders. World J. Psychiatry. 4(2), 30. http://doi.org/10.5498/wjp.v4.i2.30

Chen, S.S., Tu, P.C., Su, T.P., Hsieh, J.C., Lin, Y.C., & Chen, L.F., 2008. Impaired frontal
synchronization of spontaneous magnetoencephalographic activity in patients with
bipolar disorder. Neurosci. Lett. 445(2), 174–178.
http://doi.org/10.1016/j.neulet.2008.08.080

Duan, L., Liu, H., Wang, C., & Qiao, Y., 2021. Analysis of EEG in unipolar and bipolar
depression based on phase synchronization. 2021 4th International Conference on
Pattern Recognition and Artificial Intelligence (PRAI), 255–260.
http://doi.org/10.1109/PRAI53619.2021.9551062

Endicott, J., Nee, J., Harrison, W., & Blumenthal, R., 1993. Quality of Life Enjoyment and
Satisfaction Questionnaire: A new measure. Psychopharmacol. Bull. 29(2), 321–326.

Fu, C.H.Y., & Costafreda, S.G., 2013. Neuroimaging-based biomarkers in psychiatry: clinical
opportunities of a paradigm shift. Can. J. Psychiatry. 58(9), 499–508.
http://doi.org/10.1177/070674371305800904

Ghazi-Noori, A-R., Woodham, R.D., Rezaei, H., Sharif, M.S., Bramon, E., Ritter, P., Bauer, M.,
Young, A.H., & Fu, C.H.Y., 2024. Home-based transcranial direct current stimulation in
bipolar depression: an open-label treatment study of clinical outcomes, acceptability and
adverse events. Int. J. Bipolar Disord. 12, 30. https://doi.org/10.1186/s40345-024-00352-
9

Grimm, S., Beck, J., Schuepbach, D., Hell, D., Boesiger, P., Bermpohl, F., Niehaus, L., Boeker, H., & Northoff, G., 2008. Imbalance between left and right dorsolateral prefrontal cortex in major depression is linked to negative emotional judgment: an fMRI study in severe major depressive disorder. Biol. Psychiatry. 63(4), 369–376. https://doi.org/10.1016/j.biopsych.2007.05.033

Hamilton, M., 1959. The assessment of anxiety states by rating. Br. J. Med. Psychol. 32(1), 50–55. https://doi.org/10.1111/j.2044-8341.1959.tb00467.x

Hamilton, M., 1960. A rating scale for depression. J. Neurol. Neurosurg. Psychiatry. 23(1), 56–62. https://doi.org/10.1136/jnnp.23.1.56

Harmony, T., 2013. The functional significance of delta oscillations in cognitive processing. Front. Integr. Neurosci. 7, 83. https://doi.org/10.3389/fnint.2013.00083

Hassel, S., Almeida, J.R.C., Kerr, N., Nau, S., Ladouceur, C.D., Fissell, K., Kupfer, D.J., & Phillips, M.L., 2008. Elevated striatal and decreased dorsolateral prefrontal cortical activity in response to emotional stimuli in euthymic bipolar disorder: no associations with psychotropic medication load. Bipolar Disord. 10(8), 916–927. https://doi.org/10.1111/j.1399-5618.2008.00641.x

Kam, J.W.Y., Bolbecker, A.R., O'Donnell, B.F., Hetrick, W.P., & Brenner, C.A., 2013. Resting state EEG power and coherence abnormalities in bipolar disorder and schizophrenia. J. Psychiatr. Research. 47(12), 1893–1901. http://doi.org/10.1016/j.jpsychires.2013.09.009

Kim, D-J., Bolbecker, A.R., Howell, J., Rass, O., Sporns, O., Hetrick, W.P., Breier, A., & O'Donnell, B.F., 2013. Disturbed resting state EEG synchronization in bipolar disorder: a graph-theoretic analysis. NeuroImage Clin. 2, 414–423. http://doi.org./10.1016/j.nicl.2013.03.007

Krigolson, O.E., Hammerstrom, M.R., Abimbola, W., Trska, R., Wright, B.W., Hecker, K.G., & Binsted, G., 2021. Using Muse: Rapid mobile assessment of brain performance. Front. Neurosci. 15, 634147. https://doi.org/10.3389/fnins.2021.634147

Kroenke, K., Spitzer, R., & Williams, W., 2001. The PHQ-9: Validity of a brief depression severity measure. J. Gen. Intern. Med. 16, 606–616. http://doi.org/10.1046/j.1525-1497.2001.016009606.x

Kunze, T., Hunold, A., Haueisen, J., Jirsa, V., & Spiegler, A., 2016. Transcranial direct current stimulation changes resting state functional connectivity: A large-scale brain network modeling study. Neuroimage. 140, 174–187. https://doi.org/10.1016/j.neuroimage.2016.02.015

Lee, J., Lee, C. W., Jang, Y., You, J.S., Park, Y.S., Ji, E., Yu, H., Oh, S., Ryoo, H.A., Cho, N., Park, J.Y., Yoon, J., Baek, J.H., Park, H.Y., Ha, T.H., & Myung, W. (2022). Efficacy and safety of daily home-based transcranial direct current stimulation as adjunct treatment for bipolar depressive episodes: Double-blind sham-controlled randomized clinical trial. Front. Psychiatry. 13, 969199. https://doi.org/10.3389/fpsyt.2022.969199

Maeda, F., Keenan, J.P., & Pascual-Leone, A., 2000. Interhemispheric asymmetry of motor cortical excitability in major depression as measured by transcranial magnetic stimulation. Br. J. Psychiatry. 177(2), 169–173. https://doi.org/10.1192/bjp.177.2.169

McIntyre, R.S., Alda, M., Baldessarini, R.J., Bauer, M., Berk, M., Correll, C.U., Fagiolini, A., Fountoulakis, K., Frye, M.A., & Grunze, H., 2022. The clinical characterization of the adult patient with bipolar disorder aimed at personalization of management. World Psychiatry. 21(3), 364–387. http://doi.org/10.1002/wps.20997

Mitoma, R., Tamura, S., Tateishi, H., Mitsudo, T., Tanabe, I., Monji, A., & Hirano, Y., 2022. Oscillatory brain network changes after transcranial magnetic stimulation treatment in

patients with major depressive disorder. J. Affect. Disord. Rep. 7, 100277.

https://doi.org/10.1016/j.jadr.2021.100277

Montgomery, S.A., & Åsberg, M., 1979. A new depression scale designed to be sensitive to

change. Br. J. Psychiatry. 134(4), 382–389.

Mutz, J., Vipulananthan, V., Carter, B., Hurlemann, R., Fu, C.H.Y., & Young, A.H., 2019.

Comparative efficacy and acceptability of non-surgical brain stimulation for the acute

treatment of major depressive episodes in adults: systematic review and network meta-

analysis. Bmj. 364. https://doi.org/10.1136/bmj.l1079

Nikolin, S. et al. Time-course of the tDCS antidepressant effect: An individual participant data

meta-analysis. Prog. Neuropsychopharmacol. Biol. Psychiatry 125, 110752 (2023).

https://doi.org/10.1016/j.pnpbp.2023.110752

Pellegrino, G., Maran, M., Turco, C., Weis, L., di Pino, G., Piccione, F., & Arcara, G., 2018.

Bilateral transcranial direct current stimulation reshapes resting-state brain networks: a

magnetoencephalography assessment. Neural Plast. 2018, 2782804

https://doi.org/10.1155/2018/2782804

Polanía, R., Nitsche, M.A., & Paulus, W., 2011. Modulating functional connectivity patterns and

topological functional organization of the human brain with transcranial direct current

stimulation. Hum. Brain Mapp. 32(8), 1236–1249. http://doi.org/10.1002/hbm.21104

Quirk, G.J., Likhtik, E., Pelletier, J.G., & Paré, D., 2003. Stimulation of medial prefrontal cortex

decreases the responsiveness of central amygdala output neurons. J. Neurosci. 23(25),

8800–8807. https://doi.org/10.1523/JNEUROSCI.23-25-08800.2003

Rimmer, R.M., Woodham, R.D., Cahill, S., & Fu, C.H.Y., 2024. Acceptability of home-based

transcranial direct current stimulation (tDCS) in major depression: A qualitative analysis

of individual experiences. Ment. Health Rev. J. 29(1), 79–91.

https://doi.org/10.1108/MHRJ-07-2022-0050

Sheehan, D.V., 1893. The Sheehan Disability Scales. In The Anxiety Disease and How to

Overcome It (p. 151). Charles Scribner and Sons.

Sheehan, D.V, Lecrubier, Y., Sheehan, K.H., Amorim, P., Janavs, J., Weiller, E., Hergueta, T.,

Baker, R., & Dunbar, G.C., 1998. The Mini-International Neuropsychiatric Interview

(MINI): the development and validation of a structured diagnostic psychiatric interview for

DSM-IV and ICD-10. J. Clin. Psychiatry. 59(20), 22–33.

Siegel-Ramsay, J.E., Bertocci, M.A., Wu, B., Phillips, M.L., Strakowski, S.M., & Almeida, J.R.C.,

2022. Distinguishing between depression in bipolar disorder and unipolar depression

using magnetic resonance imaging: a systematic review. Bipolar Disorders. 24(5), 474–

498. https://doi.org/10.1111/bdi.13176

Squarcina, L., Villa, F.M., Nobile, M., Grisan, E., & Brambilla, P., 2021. Deep learning for the

prediction of treatment response in depression. J. Affect. Disord. 281, 618–622.

https://doi.org/10.1016/j.jad.2020.11.104

Stagg, C.J., Antal, A., & Nitsche, M.A., 2018. Physiology of transcranial direct current

stimulation. J. ECT. 34(3), 144–152. http://doi.org/10.1097/YCT.0000000000000510

Tortella, G., Casati, R., Aparicio, L.V.M., Mantovani, A., Senço, N., D'Urso, G., Brunelin, J.,

Guarienti, F., Selingardi, P.M.L., & Muszkat, D., 2015. Transcranial direct current

stimulation in psychiatric disorders. World J. Psychiatry. 5(1), 88.

http://doi.org/10.5498/wjp.v5.i1.88

Townsend, J., Bookheimer, S.Y., Foland–Ross, L.C., Sugar, C.A., & Altshuler, L.L., 2010. fMRI

abnormalities in dorsolateral prefrontal cortex during a working memory task in manic,

euthymic and depressed bipolar subjects. Psychiatry Res. Neuroimaging. 182(1), 22–29. https://doi.org/10.1016/j.pscychresns.2009.11.010

Tzagarakis, C., Ince, N.F., Leuthold, A.C., & Pellizzer, G., 2010. Beta-band activity during motor planning reflects response uncertainty. J. Neurosci. 30(34), 11270–11277. http://doi.org/10.1523/JNEUROSCI.6026-09.2010

Woodham, R.D., Selvaraj, S., Lajmi, N., Hobday, H., Sheehan, G., Ghazi-Noori, A-R., Lagerberg, P.J., Rizvi, M., Kwon, S.S., Orhii, P., Maislin, D., Hernandez, L., Machado-Vieira, R., Soares, J.C., Young, A.H., & Fu, C.H.Y., 2023. Home-based transcranial direct current stimulation RCT in major depression [Preprint]. https://doi.org/10.1101/2023.11.27.23299059

Woodham, R., Rimmer, R.M., Mutz, J., & Fu, C.H.Y., 2021. Is tDCS a potential first line treatment for major depression? Int. Rev. Psychiatry. 33(3), 250–265. https://doi.org/10.1080/09540261.2021.1879030

Woodham, R.D., Rimmer, R.M., Young, A.H., & Fu, C.H.Y., 2022. Adjunctive home-based transcranial direct current stimulation treatment for major depression with real-time remote supervision: An open-label, single-arm feasibility study with long term outcomes. J. Psychiatr. Res. 153, 197–205. https://doi.org/10.1016/j.jpsychires.2022.07.026

Woźniak-Kwaśniewska, A., Szekely, D., Harquel, S., Bougerol, T., & David, O., 2015. Resting electroencephalographic correlates of the clinical response to repetitive transcranial magnetic stimulation: a preliminary comparison between unipolar and bipolar depression. J. Affect. Disord.183, 15–21. http://doi.org/10.1016/j.jad.2015.04.029

Young, R.C., Biggs, J.T., Ziegler, V.E., & Meyer, D.A., 1978. A rating scale for mania: Reliability, validity and sensitivity. Br. J. Psychiatry. 133(5), 429–435. https://doi.org/10.1192/bjp.133.5.429

Zhang, Y., Chen, Y., Bressler, S.L., & Ding, M., 2008. Response preparation and inhibition: the role of the cortical sensorimotor beta rhythm. Neuroscience. 156(1), 238–246. http://doi.org/10.1016/j.neuroscience.2008.06.061

Zuchowicz, U., Wozniak-Kwasniewska, A., Szekely, D., Olejarczyk, E., & David, O., 2019. EEG phase synchronization in persons with depression subjected to transcranial magnetic stimulation. Front. Neurosci. 12, 430602. http://doi.org/10.3389/fnins.2018.01037

Figure Legends

Figure 1.

Image of (a) EEG device (Muse), which consisted of four electrode (AF7, AF8, TP9 and TP10), and (b) EEG distribution of electrodes based on international 10/20 positioning.

Figure 2.

Image representing averaged PLV values across different group (remission and non-remission group) and time (pre- and post-treatment). Rows depict EEG bands: full band, delta, theta, alpha, beta and gamma, and columns represent participant categories: pre-treatment remission, pre-treatment non-remission, post-treatment remission, and post-treatment non-remission groups.

Figure 3.

Scatter plots of phase locking value (PLV) (y-axis: Difference in EEG) of variables showing significant positive correlation with proportional change in MADRS (x-axis: Difference in MADRS) across participants. Positive correlations were observed for each PLV synchronization EEG channel pair.

Figure 4.

Boxplots comparing phase locking values (PLV) between remission and non-remission groups within specific frequency bands. The remission group exhibited increased PLV as compared to the non-remission group post-treatment across electrode pairs within delta, theta, alpha and gamma frequency ranges. Significant differences are denoted by *, indicating adjusted p-values corrected for false discovery rate (FDR) below 0.05. Purple colour signifies the remission group, and green indicates the non-remission group. Significant main effects for groups in the PLV of AF7-TP9 were found across the full, alpha, and beta bands, in which post-hoc tests showed significant differences between groups at post-treatment. Remission group showed increased PLV value as compared to the non-remission group at post-treatment, including PLV of AF7 and AF8 in delta, theta and alpha bands (U_{delta} = 80.00, FDR-adjusted p = 0.02; U_{theta} = 81.00, FDR-adjusted p = = 0.02; U_{alpha} = 87.00, FDR-adjusted p = .000); PLV of AF7 and TP10 in delta and alphaband (U_{delta} = 77.00, FDR-adjusted p = 0.04; U_{alpha} = 76.00, FDR-adjusted p = 0.04); PLV

of TP9 and TP10 in delta and theta bands (U_{delta} = 79.00, FDR-adjusted p = 0.03; U_{theta} = 81.00, FDR-adjusted p = 0.02) .

Figure 5.

Comparative boxplot of phase locking value (PLV) of TP9 and TP10 at beta band between remission and non-remission groups.

Table 1.
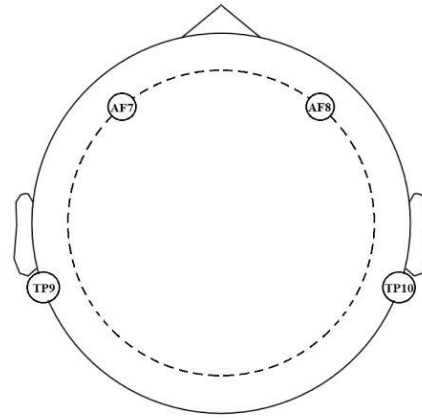**Demographic characteristics of participants**

Characteristic	Remission	Non-Remission
Total number (women)	11 (9)	9 (5)
Age	47.19 ± 12.15	55.11 ± 6.05
Years of education	17.82 ± 1.94	15.67 ± 2.18
IQ	102.55 ± 9.17	102.89 ± 7.62
Duration current depressive episode (weeks)	54.45 (3-260)	92.56 (8-64)
Clinical assessments scores at baseline		
MADRS	24.00 ± 3.13	26.89 ± 2.15
HDRS-17	19.45 ± 2.11	19.78 ± 2.54
HAMA	15.00 ± 4.98	16.56 ± 3.71
YMRS	2.73 ± 1.27	3.22 ± 1.72
PHQ-9	15.73 ± 4.36	18.67 ± 3.16
SDS	19.55 ± 8.03	21.89 ± 6.11
Clinical assessments scores at end of treatment		
MADRS	5.18 ± 1.72	14.40 ± 4.88
HDRS-17	3.55 ± 1.44	10.56 ± 5.00
HAMA	3.82 ± 1.66	10.33 ± 4.06
YMRS	0.64 ± 1.03	1.33 ± 1.22
PHQ-9	5.27 ± 3.04	10.56 ± 5.22
SDS	8.64 ± 6.28	17.11 ± 6.47
Treatments during trial		
Taking mood stabilizer and other medications	10	6
Taking antidepressant medication only	0	1
Taking no medication	1	2
Engaged in psychotherapy	4	1

Categorical variables are presented as number of participants with percentage in parentheses for treatments during trial. Duration current depressive episode is presented as mean with range in parentheses. Mean values are presented with '±' standard deviation values. MADRS, Montgomery-Åsberg Depression Rating Scale; HDRS-17, 17-item Hamilton Depression Rating Scale; HAMA, Hamilton Anxiety Rating Scale; YMRS, Young Mania Rating Scale; PHQ-9, Patient Health Questionnaire-9; SDS, Sheehan Disability Scale. There is no significant difference between remission and non-remission group at age (t = -1.896, p = 0.077) or gender (x^2 = 0.616, p = 0.433). However, there is a significant difference at the baseline MADRS score (t = -2.365, p = 0.030), and at week 6 post-treatment (t = -5.429, p < 0.001).
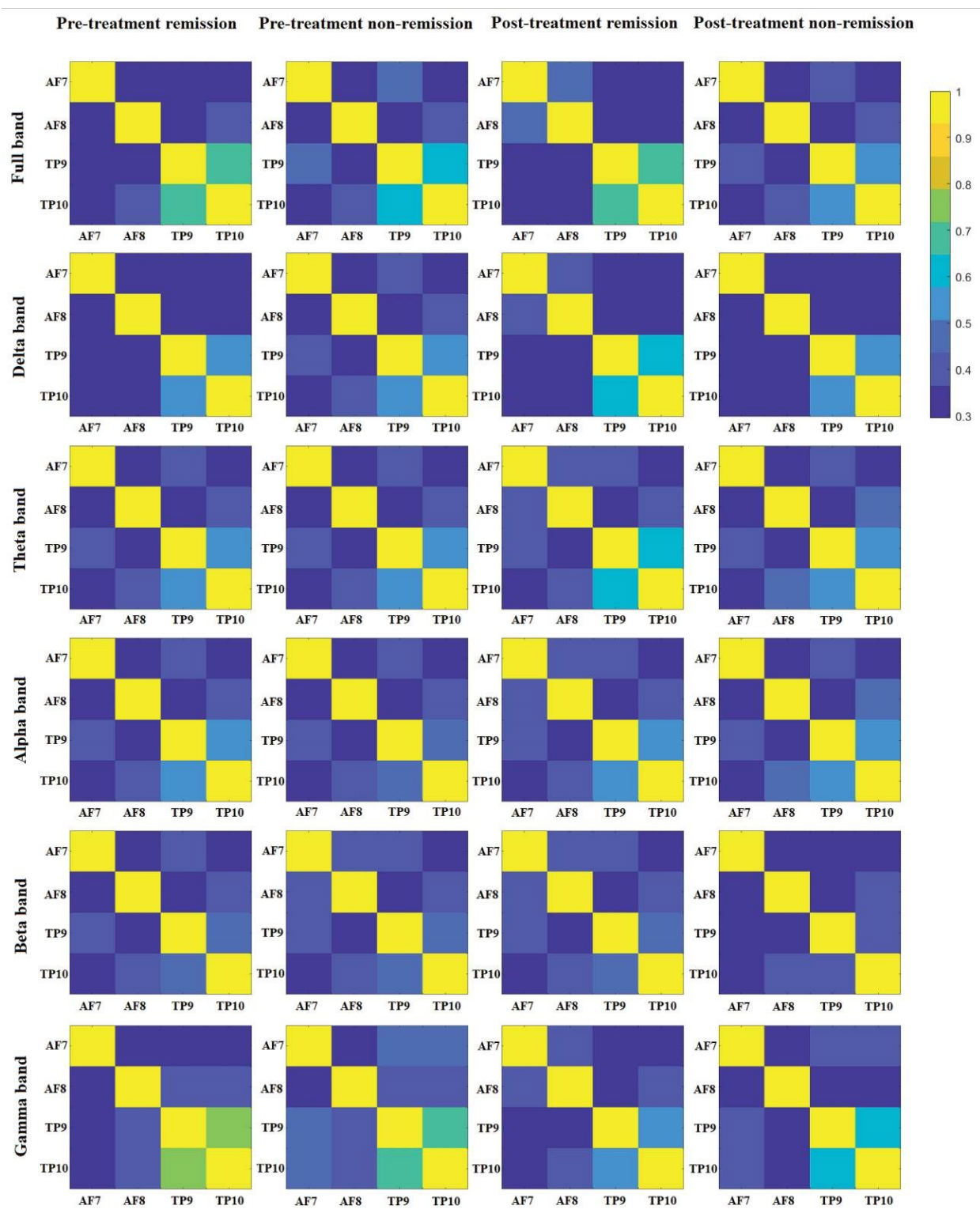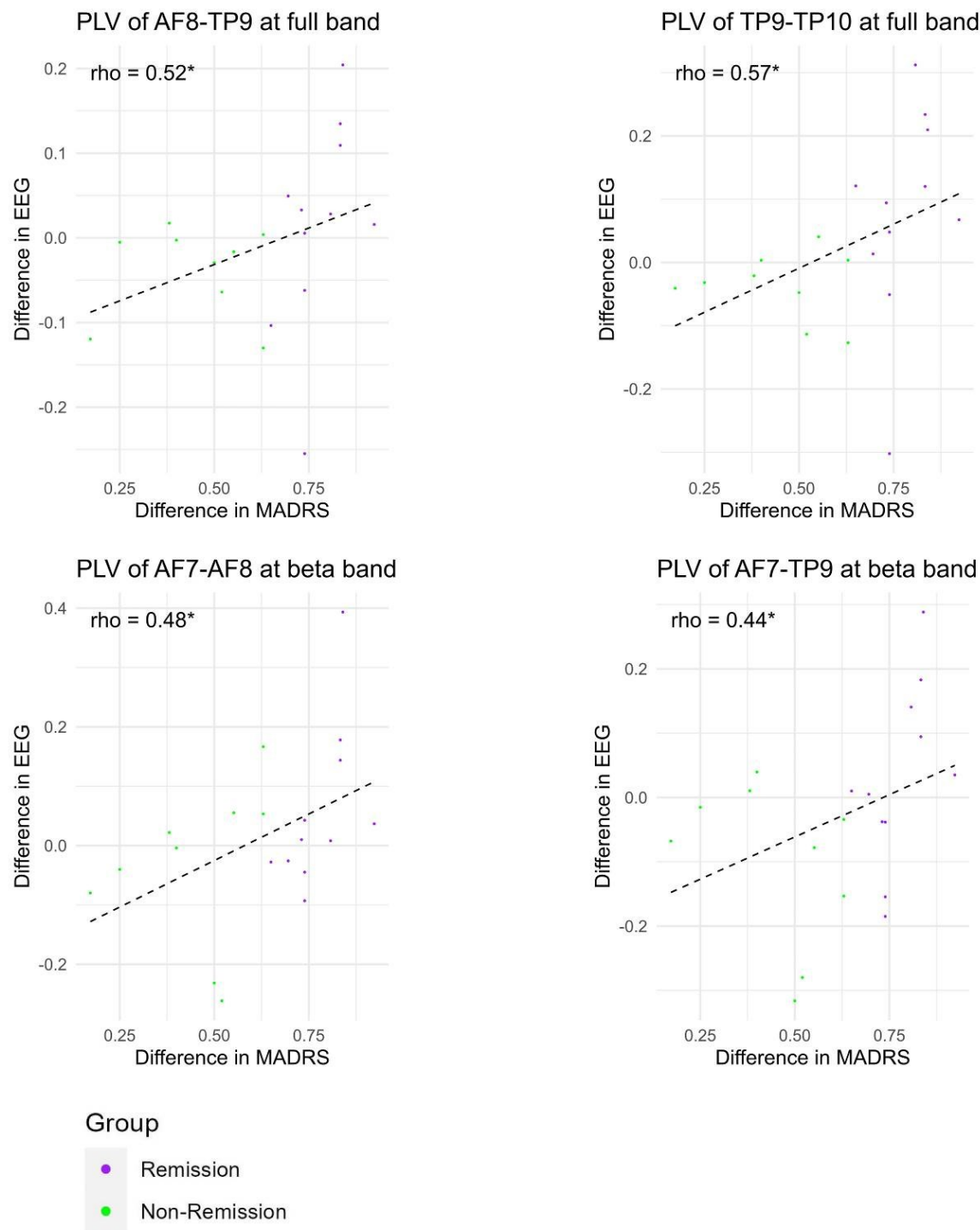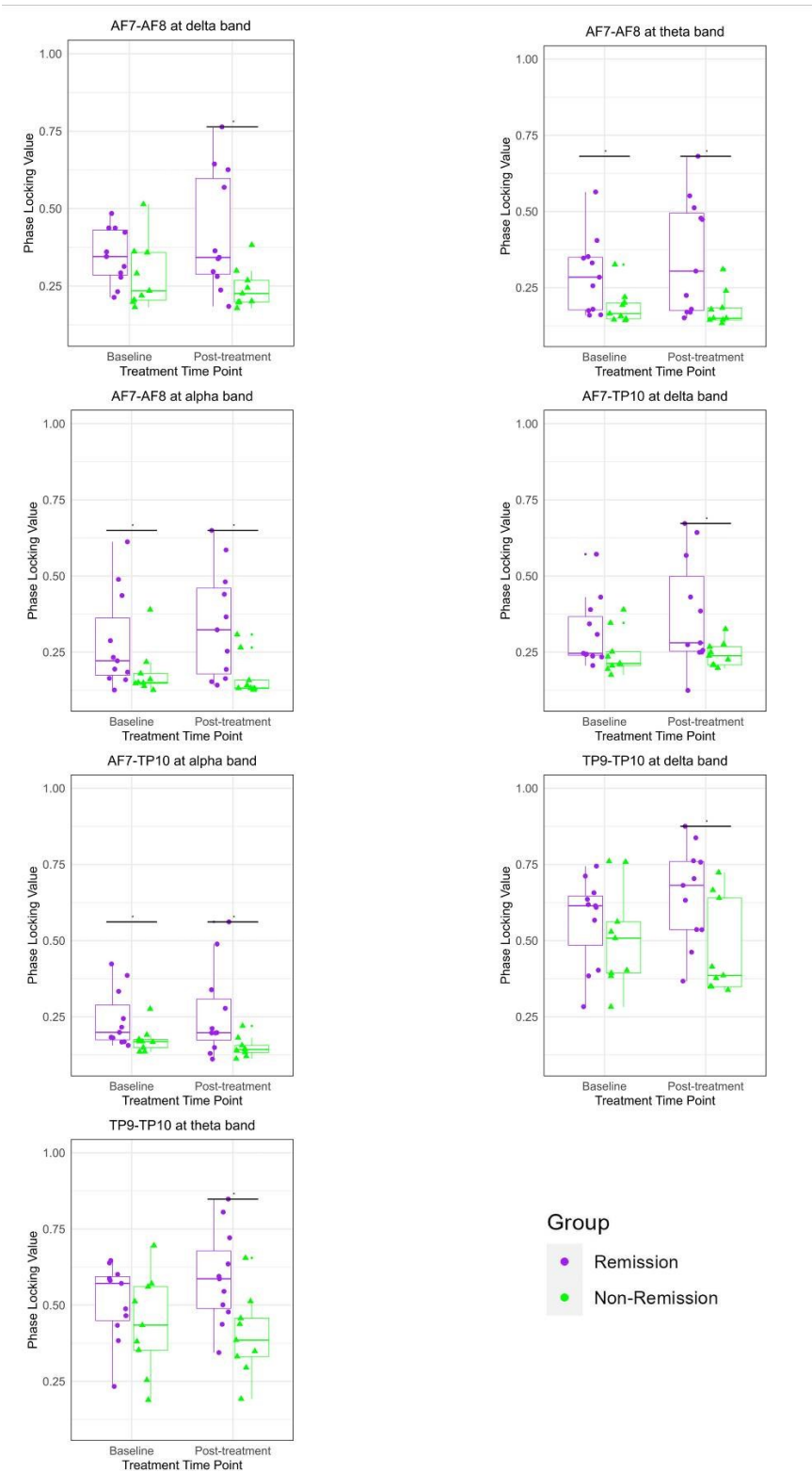
Figure 1.

(a)

(b)

Figure 2.

Figure 3.

PLV of AF8-TP9 at full band

rho = 0.52*

PLV of TP9-TP10 at full band

rho = 0.57*

PLV of AF7-AF8 at beta band

rho = 0.48*

PLV of AF7-TP9 at beta band

rho = 0.44*

Group
- Remission
- Non-Remission

Figure 4.

Figure 5.

TP9-TP10 at beta band